# Textural and Compositional Variability Across Littoral Segments of Lake Tanganyika: The Effect of Asymmetric Basin Structure on Sedimentation in Large Rift Lakes[1]

Michael J. Soreghan[2] and Andrew S. Cohen[3]


## ABSTRACT

Lake Tanganyika, part of the East African rift system, represents one of the most widely cited modern analogs for interpreting ancient rift lakes. To date, few published detailed sedimentologic studies of the modern sediments allow for comparisons to outcrop- and well-bore-scale observations within ancient strata.

Four recurrent structural margin types exist along the alternating half-graben structure of the lake: hinged margins, axial margins, accommodation zone margins, and escarpment margins. The hinged margin consists of a series of structurally controlled benches over which long, continuous tracts of bioclastic lag deposits predominate; clastic sands are limited to moderate-size silty deltas and long, narrow shoreface sands. The axial margin is dominated by a wave-dominated, silt-rich delta system. Accommodation zone margins consist of bioclastic lag deposits atop structural highs, whereas carbonate and clastic mud accumulates farther offshore. Escarpment margins contain small fan-delta deposits alternating along shore with talus deposits; offshore carbonate and clastic mud is present away from active gravity-flow deposition. Total organic carbon (TOC) and pyrolysis data from fine-grained samples subtly reflect the contrasts in margin types, but these values are controlled more directly by water depth.

Although facies are similar among all margin types, their spatial distribution, in particular the degree to which facies tracts trend parallel to shore, best discriminates among the different margin types. These data suggest that unique but predictable associations of reservoir, seal, and source facies exist along each of the different margin types.


## INTRODUCTION

Thick lacustrine strata commonly form a significant component of both ancient and modern rift basins. Typically, lacustrine deposits exhibit abrupt vertical and lateral facies changes, producing a complex three-dimensional facies geometry. Both the episodic tectonism of rifts and the climate-induced fluctuations in the water budget of the rift basin control this facies complexity. Nevertheless, differentiating the controls on facies distributions in rift lakes is an important goal because rift lakes not only represent viable economic targets for hydrocarbons and other mineral deposits, but also form long-term repositories of paleoclimatic data for continental regions.

Numerous structural and reflection seismic studies within the East African rift confirm that the rift evolved in an asymmetric fashion (Rosendahl et al., 1986; Ebinger, 1989a; Sander and Rosendahl, 1989). Consequently, recent models developed for sedimentation within rifts incorporate a half-graben



[1]Manuscript received January 17, 1995; revised manuscript received August 2, 1995; final acceptance November 2, 1995.

[2]Department of Geosciences, University of Arizona, Tucson, Arizona 85721. Present Address: School of Geology and Geophysics, Sarkeys Energy Center, 100 E. Boyd Street, University of Oklahoma, Norman, Oklahoma 73019.

[3]Department of Geosciences, University of Arizona, Tucson, Arizona 85721.

This study represents part of Soreghan's Ph.D. dissertation at the University of Arizona and benefited from assistance from numerous people there and elsewhere. We appreciate the assistance of Gaspard Ntakimazi, Laurent Ntahuga, Pontien Ndabaneze, and others at the Faculté des Sciences, Université du Burundi, for logistical support while in Africa. In addition, Jean-Jacques Tiercelin and Köen Marten provided monetary and technical support during a joint project in 1992. D. Gevirtzman, B. Hussein, M. Johnston, R. Jones, E. Michel, E. Mkoni, G. Soreghan, and K. West provided valuable assistance in data-collection support over various field seasons at Lake Tanganyika. We would like to acknowledge Harry Dembicki of Marathon Oil Company who provided Rock-Eval pyrolysis analyses for a suite of samples. We are indebted to Lisa Pratt of the Organic Geochemistry Lab of Indiana University who provided laboratory facilities for TOC and acid-insoluble sulfur analyses. Conversations with C. Scholz, T. Johnson, and J. J. Tiercelin helped shape some of our ideas. Earlier versions of this manuscript were improved by comments from C. G. Chase, W. R. Dickinson, J. T. Parrish, J. F. Schreiber, Jr., and G. S. Soreghan, and by AAPG reviewers A. J. Lomando, C. K. Morley, and W. A. Wescott. This work was partially funded by grants from Amoco Production Company, Conoco Inc., Marathon Oil Company, the National Undersea Research Council, and the H. M. Keck Foundation, as well as grants from AAPG, the Geological Society of America, and the University of Arizona.

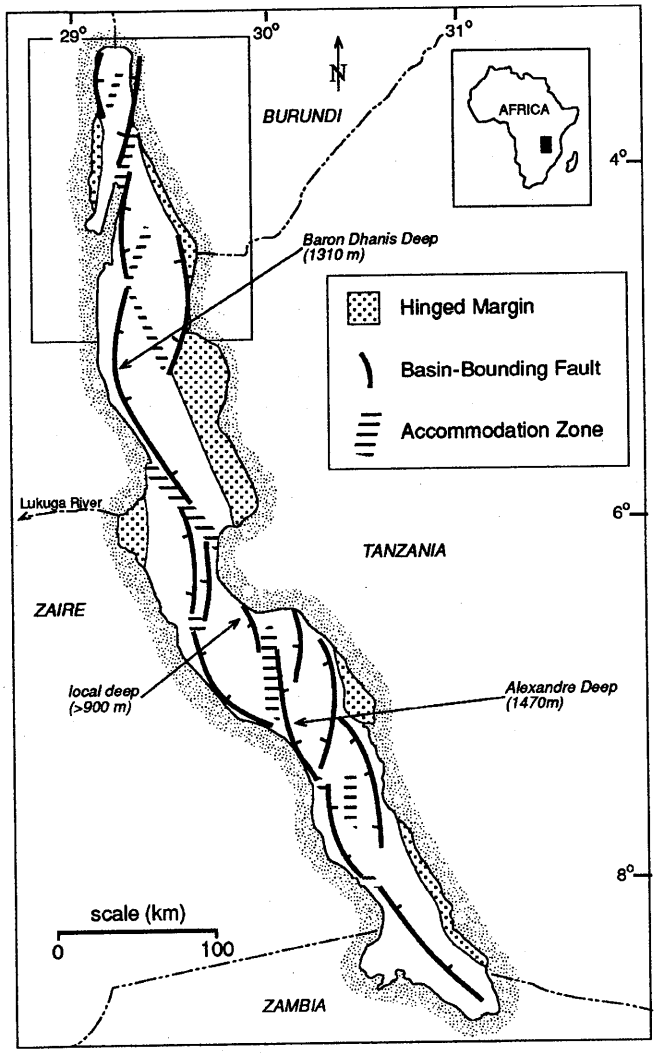


**Figure 1—Generalized tectonic map of Lake Tanganyika emphasizing the alternating, half-graben morphology of the basin. Hachures on faults are on side of the downthrown block. The box at the northern end of the lake outlines the study area shown in Figure 3. Structure simplified from Rosendahl et al. (1986), Morley (1988), and Ebinger (1989a).**

geometry as one variable that controls deposition (Turner-Peterson and Smoot, 1985; Leeder and Gawthorpe, 1987; Blair and Bilodeau, 1988; Burgess et al., 1988; Gore, 1988; Cohen, 1989, 1990; Lambiase, 1990; Scholz and Rosendahl, 1990; Scholz et al., 1990; Tiercelin et al., 1992). For example, Cohen (1990) developed a tectonic-stratigraphic model for rift lake deposits based on general observations from Lake Tanganyika. Tiercelin et al. (1992) followed with a study that incorporated high-resolution seismic and core data to develop a similar model. Other models have been developed from a combination of several East African lakes and other rift systems to predict basin-fill patterns (Lambiase, 1990; Scholz and Rosendahl, 1990; Scholz et al., 1990; Lambiase and Bosworth, 1994). To date, however, few quantitative sedimentologic studies document the extent of facies differences created by the structural asymmetry within modern rift lakes [exceptions include Cohen et al. (1986), Yuretich (1986), Owen and Crossley (1989), Johnson and Ng'ang'a (1990), and Johnson et al. (1995)].

The goal of this study is to document facies patterns and the distribution of organic matter across specific shallow-water regions of northern Lake Tanganyika, Africa, that represent the typical structural lake margins found within asymmetric East African lake basins. From these data we quantitatively compare and contrast characteristics of sedimentation among different structural margins of the lake to document the variables most sensitive to the half-graben structure of the basin. The results of this study contribute to an improved understanding of the relationship between facies patterns and paleogeography of rift basins by providing data comparable to borehole- or outcrop-based data from ancient rift lake stratigraphic sequences.

## BACKGROUND

### Regional Tectonic Setting

Lake Tanganyika lies within the western arm of the East African rift system (McConnell, 1972; Ebinger, 1989a). The initiation of rifting and attendant basin formation was probably diachronous throughout the rift and is not well constrained, but may be between 9 and 12 Ma (Cohen et al., 1993), although other workers suggest a significantly older age (16–24 Ma) (Burgess et al., 1988; Tiercelin and Mondeguer, 1991).

A series of half-graben basins, 80–160 km long and 30–80 km wide, comprise the Lake Tanganyika basin. In this geometry, border-fault segments typically face opposite directions along the rift axis (Figure 1) (Rosendahl et al., 1986; Morley, 1988; Ebinger, 1989a; Sander and Rosendahl, 1989). Accommodation zones (transfer zones of Nelson et al., 1992) are structural horsts that trend roughly 45 to 60° from the rift axis and provide for differential subsidence between two adjacent half-grabens (Rosendahl et al., 1986; Ebinger, 1989b; Morley et al., 1990; Nelson et al., 1992). Maximum sedimentary fill within local depocenters of Lake Tanganyika exceeds 6 km (Burgess et al., 1988; Tiercelin and Mondeguer, 1991; Cohen et al., 1993), and elevation along border-fault segments ranges between 1 and 3 km above lake level (Ebinger, 1989a), producing structural relief of at least 7–9 km.

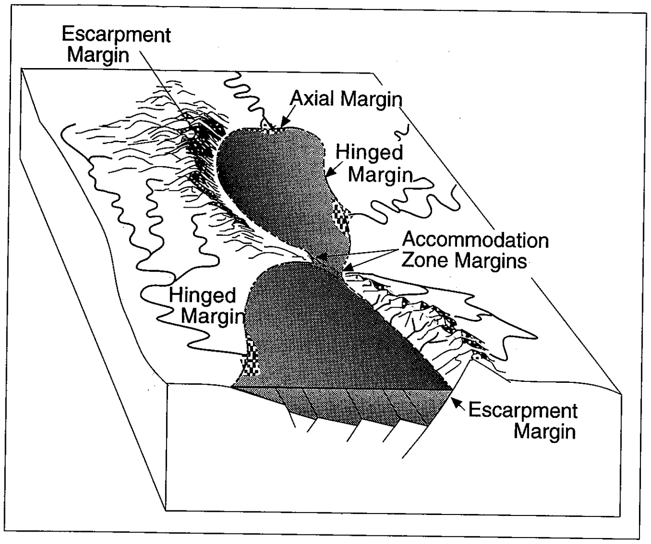


**Figure 2—Block diagram illustrating structural margin types present within an alternating half-graben lake basin. These margin types are the focus of this study.**

The structural complexity of Lake Tanganyika produces a highly asymmetric and variable basin morphology. Capart (1949) first showed that the three deepest points of Lake Tanganyika lie just offshore and not within the center of the lake (Figure 1). The nature of the shoreline and the littoral zone bathymetry also changes abruptly as the shoreline passes from one structural margin to another. Figure 2 depicts the terminology used in this study for the distinct lake margin types that result from the alternating half-graben morphology: (1) escarpment margins lie adjacent to border faults; (2) hinged margins lie on the lakeshore opposite border faults; (3) accommodation zone margins lie across the complex horst blocks/fault zones that separate half grabens; and (4) axial margins lie where the lake margin trends approximately perpendicular to the rift axis. This terminology varies slightly from that of Tiercelin et al. (1992), but follows closely that of Cohen (1990) and Rosendahl et al. (1986).

## Climate and Hydrology

Lake Tanganyika has an area of 33,000 km$^2$, a maximum depth of 1470 m, and lies within the tropical subhumid belt. Precipitation within the Lake Tanganyika basin ranges from 800 to 1200 mm/yr and falls primarily during two rainy seasons (September–November and February–April). During the remaining months the region is drier and experiences intensified southerly winds. Presently, the lake is hydrologically open (through the Lukuga River, Zaire; Figure 1), although 90% of the water loss occurs through evaporation from the lake surface (Coulter and Spigel, 1991). Influent waters generally form strong underflows upon entering the lake because they are typically cold and highly charged with suspended sediment, especially during the rainy season.

The lake is thermally stratified with permanently anoxic waters below 80–250 m water depth (Hecky and Degens, 1973; Coulter and Spigel, 1991). The thermocline ranges between approximately 50 and 120 m depth. Water temperatures within the mixed, upper waters (epilimnion) range between 24° and 27°C, becoming constant at 23.2° to 23.5°C within the stable, permanently anoxic bottom waters (hypolimnion). The lake waters are fresh (salinity = 0.5‰) and mildly alkaline (pH = 9.15 ±0.05) with a high (~4:1) Mg:Ca ratio (Casanova and Hillaire-Marcel, 1992). The most important source of nutrients for primary productivity is internal recycling within the lake during the dry, windy season; riverine input is minor (Huc et al., 1990).

## METHODS

We investigated six study sites (Figure 3): (1) Ruzizi River delta, Burundi (axial margin); (2) Nyanza Lac, Burundi (hinged margin); (3) Magara, Burundi (accommodation zone margin); (4) Cape Banza, Zaire (accommodation zone margin); (5) Bemba, Zaire (escarpment margin); and (6) Kigoma, Tanzania (escarpment margin). Each site represents one of the four margin types and incorporates the entire zone from the shoreline to an offshore distance well into the anoxic zone. Each site ranges in area from 5 to 80 km$^2$ depending upon the bathymetric gradients and the heterogeneity of depositional subenvironments.

We conducted a bathymetric survey at each site using a single-channel Lowrance X-16 sonar system with an 8° transducer, typically mounted on a small, inflatable boat. Sonar transects provided the data for the bathymetric maps used in this study and allowed us to identify features relevant to the sedimentology of the site (e.g., channels or submerged rocky outcrops).

We collected a total of 320 samples by use of one of three methods: (1) a modified Eckman corer; (2) a "scooper" sampler; and (3) by hand using scuba divers. The sampling scheme at each site was a nonuniform grid that was biased toward regions of transitions between subenvironments. We employed scuba divers for direct observation at each site in depths of less than 40 m for documentation of facies relationships to supplement the laboratory analyses of boat-collected samples.

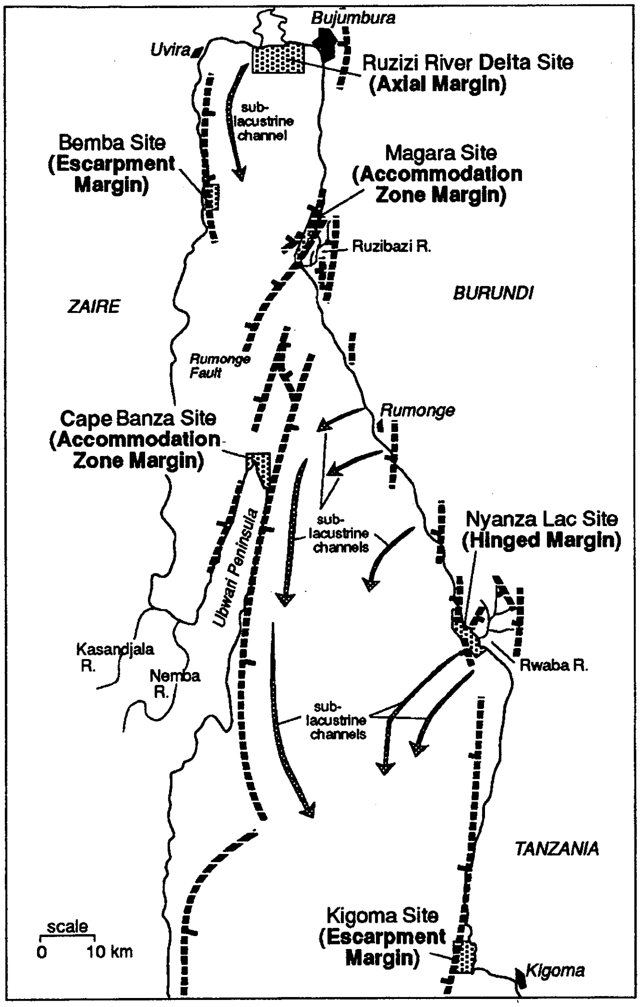


**Figure 3—Location map highlighting study sites. Fault pattern is simplified from Morley (1988) and Ebinger (1989a). Locations of modern sublacustrine channels and canyons are taken from Tiercelin et al. (1992).**

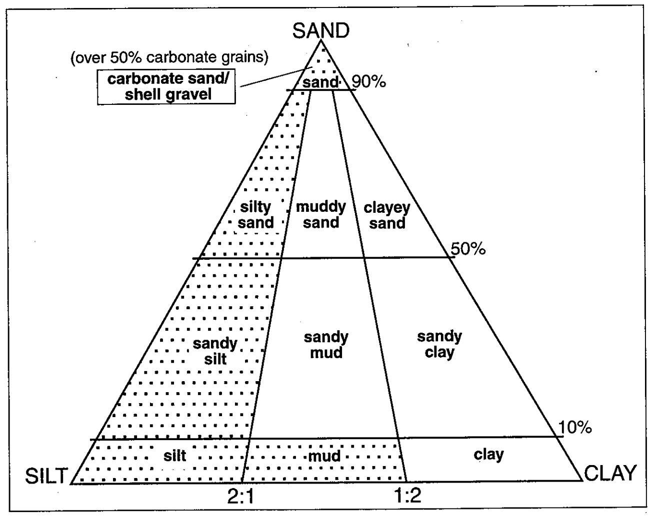


**Figure 4—Ternary plot of relative percentage of sand, silt, and clay with classification of textural facies from Folk et al. (1970). Stippled regions represent facies in this study. Carbonate sand/shell gravel is texturally a sand but contains at least 50% carbonate grains. Note that silt and clay categories do not differentiate between clastic and carbonate sediments.**

After collecting the samples, we visually described them and then split them into several fractions for four types of analysis: (1) granulometry; (2) carbon/sulfur; (3) Rock-Eval pyrolysis; and (4) composition. We performed granulometric analyses using standard methods outlined in Lewis (1984). For those samples with more than 10% mud, we analyzed the mud fraction with a CILAS 715 Granulometer located at the University of California-Davis. We analyzed 130 representative samples for total carbon (TC), total organic carbon (TOC), total sulfur (TS), and acid-insoluble sulfur (insS) data using a LECO CS244, modified for high sulfur. Additionally, Rock-Eval pyrolysis was performed on separate splits of the same sample suite.

Facies were defined using the relative percentage of sand, silt, and clay following the textural classification of Folk et al. (1970) (Figure 4). In this scheme, the facies maps do not distinguish between carbonate and clastic muds. Estimates of the percentage of carbonate sediment within the mud-rich samples were inferred from TC and are described in following sections. However, because of its uniqueness, a sixth facies consisting of carbonate sand/shell gravel was defined by an abundance of bioclasts and carbonate grains (>50%) within the coarse-grained fraction (Figure 4). We further subdivided the sand facies into subfacies defined by depositional environment (beach sand facies, delta sand facies, and offshore sand facies).

## RESULTS

Table 1 summarizes granulometric data for the Lake Tanganyika sediment samples, averaged for each facies, for each of the study sites. Intersite comparisons are held to the next section; however, Figure 5 depicts the relationship between mean grain size and water depth for each site to facilitate intrasite discussions.

Tables 2 and 3 report the organic geochemical data for the Lake Tanganyika sediment samples. In both tables the data are averaged for each study site; in addition, the samples above and below 80 m water depth were averaged to test for differences in organic content between "shallow-water" and "deep-water" samples, respectively. A depth of 80 m

**Table 1. Granulometric Data for Lake Tanganyika Samples**

| Facies | Number of Samples | Mean Grain Size (ϕ) | Mean Grain Size (mm) | Sorting* (ϕ) | Skewness | Sand** (%) | Silt** (%) | Clay** (%) |
|---|---|---|---|---|---|---|---|---|
| **Nyanza Lac Site** | | | | | | | | |
| Sand | 19 | 1.80 | 0.287 | 1.43 | -0.36 | 96.7 | 3.2 | 0.2 |
| Beach sand | 5 | 1.51 | 0.351 | 0.95 | -0.17 | 99.4 | 0.6 | 0.0 |
| Delta sand | 2 | 2.33 | 0.199 | 1.30 | -0.52 | 93.4 | 6.5 | 0.1 |
| Carbonate sand/shell gravel | 12 | 1.83 | 0.281 | 1.58 | -0.46 | 96.1 | 3.7 | 0.2 |
| Silty sand | 12 | 3.04 | 0.121 | 2.01 | 0.58 | 77.0 | 20.6 | 2.4 |
| Sandy silt | 2 | 5.21 | 0.027 | 1.71 | 0.82 | 24.9 | 67.1 | 8.0 |
| Silt | 5 | 6.36 | 0.012 | 1.62 | 0.38 | 3.7 | 80.5 | 15.8 |
| **Ruzizi River Site** | | | | | | | | |
| Sand | 11 | 1.59 | 0.332 | 1.26 | 0.21 | 97.4 | 2.5 | 0.1 |
| Beach sand | 2 | 2.65 | 0.169 | 0.89 | -0.12 | 95.9 | 4.1 | 0.0 |
| Delta sand | 5 | 1.42 | 0.374 | 1.19 | 1.14 | 97.1 | 2.8 | 0.1 |
| Carbonate sand/shell gravel | 4 | 1.26 | 0.427 | 1.23 | -0.38 | 98.6 | 1.4 | 0.0 |
| Silty sand | 6 | 3.00 | 0.125 | 1.85 | 0.34 | 78.4 | 20.2 | 1.4 |
| Sandy silt | 9 | 5.11 | 0.028 | 1.64 | 0.91 | 24.4 | 68.7 | 6.9 |
| Silt | 23 | 6.38 | 0.012 | 1.57 | 0.50 | 3.6 | 80.4 | 15.9 |
| Mud | 5 | 7.36 | 0.006 | 1.85 | -0.22 | 2.9 | 54.8 | 42.3 |
| **Magara Site** | | | | | | | | |
| Sand | 19 | 1.70 | 0.308 | 1.56 | -0.48 | 97.3 | 2.5 | 0.2 |
| Beach sand | 3 | 2.19 | 0.219 | 1.05 | -0.52 | 98.5 | 1.4 | 0.1 |
| Offshore sand | 7 | 1.57 | 0.337 | 1.76 | -0.42 | 96.5 | 3.3 | 0.2 |
| Delta sand | 4 | 1.61 | 0.328 | 1.81 | -0.11 | 96.8 | 2.8 | 0.4 |
| Carbonate sand/shell gravel | 5 | 1.67 | 0.314 | 1.20 | -0.72 | 98.2 | 1.7 | 0.1 |
| Silty sand | 7 | 3.36 | 0.097 | 1.85 | 0.86 | 77.1 | 20.0 | 2.9 |
| Sandy silt | 8 | 5.11 | 0.029 | 2.01 | 0.04 | 27.7 | 63.4 | 8.9 |
| **Banza Site** | | | | | | | | |
| Sand | 12 | 1.35 | 0.392 | 1.69 | -1.04 | 98.3 | 1.7 | 0.0 |
| Beach sand | 5 | 1.19 | 0.438 | 1.65 | -1.32 | 99.2 | 0.8 | 0.0 |
| Offshore sand | 6 | 1.51 | 0.351 | 1.76 | -0.92 | 97.4 | 2.5 | 0.0 |
| Carbonate sand/shell gravel | 1 | 1.18 | 0.441 | 1.26 | -0.81 | 98.7 | 1.3 | 0.0 |
| Silty sand | 4 | 3.30 | 0.101 | 1.09 | 0.16 | 79.4 | 20.2 | 0.4 |
| Sandy silt | 2 | 5.37 | 0.024 | 1.87 | 0.62 | 26.1 | 63.3 | 10.6 |
| Silt | 11 | 6.55 | 0.011 | 1.61 | 0.37 | 2.9 | 78.4 | 18.8 |
| **Bemba Site** | | | | | | | | |
| Sand | 3 | 1.44 | 0.368 | 1.74 | 0.29 | 93.9 | 5.9 | 0.2 |
| Offshore sand | 3 | 1.44 | 0.368 | 1.74 | 0.29 | 93.9 | 5.9 | 0.2 |
| Silty sand | 4 | 3.29 | 0.102 | 1.72 | 0.40 | 72.8 | 25.9 | 1.3 |
| Sandy silt | 11 | 5.14 | 0.028 | 2.00 | -0.36 | 24.5 | 68.5 | 7.0 |
| Silt | 6 | 6.06 | 0.015 | 1.48 | 0.54 | 4.2 | 85.3 | 10.5 |
| **Kigoma Site** | | | | | | | | |
| Sand | 7 | 1.46 | 0.363 | 2.46 | 0.31 | 91.3 | 7.0 | 1.6 |
| Offshore sand | 7 | 1.46 | 0.363 | 2.46 | 0.31 | 91.3 | 7.0 | 1.6 |
| Silty sand | 1 | 2.86 | 0.138 | 1.93 | 0.24 | 72.5 | 26.1 | 1.5 |
| Sandy silt | 7 | 5.06 | 0.030 | 2.04 | 0.76 | 27.3 | 62.2 | 10.6 |
| Silt | 8 | 6.09 | 0.015 | 1.84 | 0.64 | 4.4 | 78.6 | 17.0 |

*Well sorted = <0.5; moderately well sorted = 0.5–0.8; moderately sorted = 0.8–1.4; poorly sorted = 1.4–2.0; very poorly sorted = > 2.0.
**Sand = >4ϕ; silt = 4–8ϕ; clay = <8ϕ.

was chosen because it corresponds to the uppermost limit of anoxic water within the northern part of Lake Tanganyika (Coulter and Spigel, 1991). Again, intersite comparisons will be reserved for the next section, but Figures 6 and 7 are plots of the organic data for intrasite discussion.

In the following paragraphs, we briefly describe the geomorphology and sedimentology for each

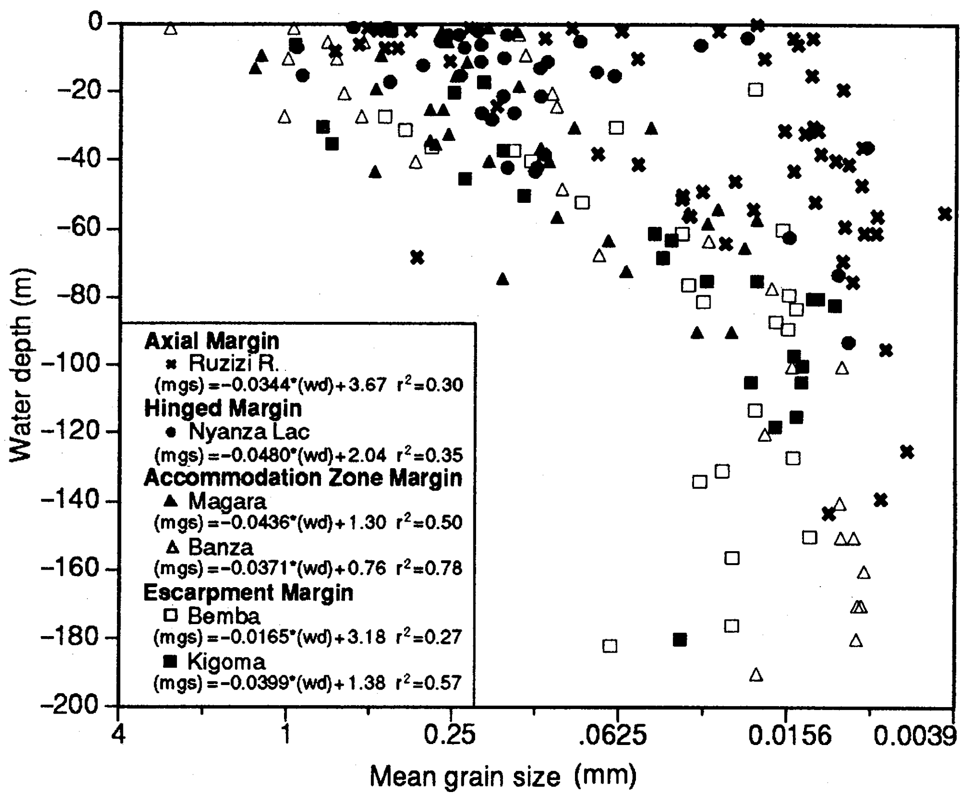


**Figure 5**—Plot of mean grain size vs. water depth of Lake Tanganyika sediment samples. Data are coded by site. Regression equations are listed in the key for each site calculated by least-squares method. mgs = mean grain size; wd = water depth. Note that independent variable (wd) is plotted on y-axis, but regression was calculated with dependent variable (mgs) on the left side of the equation.

study site; these data are presented in a series of maps that show detailed bathymetry, sample locations, transect locations, generalized onshore geomorphology, and interpreted facies patterns.

## Nyanza Lac Site: Hinged Margin

### *Geomorphology*

The Nyanza Lac, Burundi, study site lies across the lake from a large, basin-bounding normal fault (Figure 3) and therefore represents a hinged margin. The Nyanza Lac site contains only one significant perennial stream, the Rwaba River (drainage basin is 285 km$^2$). The subaerial portion of the Rwaba River delta is less than 3 km$^2$; the subaqueous delta front is less than 1 km$^2$ and exhibits a wave-dominated morphology (Coleman and Wright, 1975).

The topography and bathymetry are characterized by a stair-step morphology created by en echelon, small-scale faults (Figure 3). Onshore topography over most of the study site is subdued (30–80 m above lake level), although the terrain becomes more mountainous over the northern part of the study site (Figure 8A). The shoreline reflects these topographic differences, consisting of wide beaches in the south and rocky headlands and talus alternating with minor sandy beaches along the northern part of the study site. Offshore, the study site is dominated by a wide, low-gradient (<1°) bench that extends up to 2 km offshore and terminates at a narrow, steep (15–20°) slope (Figure 8A). The steep slope adjacent to the shoreline in the northern part of the study site flattens into another wide, low-gradient bench 80 m below lake level. One large subaqueous canyon (>20 m deep and 500 m wide) exists offshore of the Rwaba River, and smaller, narrow canyons are located offshore of the smaller streams north and south of the study site.

### *Facies Patterns*

Facies boundaries along the Nyanza Lac site coincide closely with the bathymetric changes. For example, coarse-grained facies abruptly yield to fine-grained facies at the bench–slope transition (Figure 8B). This produces a weak relationship between mean grain size and water depth ($r^2$ = 0.345; Figure 5). Carbonate sediment dominates all facies except those adjacent to and within the deltaic deposits of the Rwaba and Gifuruzi rivers.

Moderately sorted, coarse- to medium-grained mixed clastic and carbonate sand (Table 1) forms continuous beaches along the length of the study

Table 2. Means and Standard Deviations of Organic Carbon and Sulfur Contents of Lake Tanganyika Samples*

| | n | Total Carbon | | Total Sulfur | | TOC | | Acid-Insoluble Sulfur | |
|---|---|---|---|---|---|---|---|---|---|
| | | wt. % | SD | wt. % | SD | wt. % | SD | wt. % | SD |
| **All Samples by Location** | | | | | | | | | |
| Nyanza Lac | 15 | 4.72 | 2.80 | 0.06 | 0.09 | 1.13 | 0.91 | 0.04 | 0.05 |
| Ruzizi | 41 | 1.97 | 0.99 | 0.10 | 0.23 | 1.68 | 0.72 | 0.06 | 0.13 |
| Magara | 17 | 2.10 | 1.21 | 0.10 | 0.12 | 1.87 | 1.29 | 0.04 | 0.04 |
| Banza | 13 | 7.78 | 1.95 | 0.49 | 0.25 | 4.42 | 1.28 | 0.47 | 0.24 |
| Bemba | 23 | 3.10 | 1.99 | 0.21 | 0.20 | 2.77 | 1.99 | 0.14 | 0.16 |
| Kigoma | 21 | 6.13 | 2.91 | 0.27 | 0.26 | 2.48 | 1.47 | 0.15 | 0.14 |
| Magara + Banza | 30 | 4.56 | 3.25 | 0.27 | 0.27 | 3.01 | 1.81 | 0.23 | 0.27 |
| Bemba + Kigoma | 44 | 4.55 | 2.88 | 0.24 | 0.23 | 2.63 | 1.75 | 0.14 | 0.15 |
| TOTALS | 130 | 3.76 | 2.79 | 0.18 | 0.24 | 2.23 | 1.56 | 0.12 | 0.18 |
| **Samples <80 m Depth by Location** | | | | | | | | | |
| Nyanza Lac | 14 | 4.45 | 2.69 | 0.04 | 0.03 | 0.95 | 0.57 | 0.03 | 0.03 |
| Ruzizi | 37 | 1.72 | 0.51 | 0.03 | 0.05 | 1.50 | 0.48 | 0.02 | 0.02 |
| Magara | 13 | 2.02 | 1.36 | 0.05 | 0.08 | 1.77 | 1.46 | 0.02 | 0.01 |
| Banza | 2 | 4.34 | 2.20 | 0.05 | 0.03 | 1.84 | 1.18 | 0.04 | 0.03 |
| Bemba | 8 | 1.91 | 1.07 | 0.08 | 0.11 | 1.60 | 0.84 | 0.05 | 0.06 |
| Kigoma | 11 | 4.02 | 2.19 | 0.15 | 0.21 | 1.47 | 1.05 | 0.10 | 0.12 |
| Magara + Banza | 13 | 2.33 | 1.61 | 0.05 | 0.07 | 1.78 | 1.38 | 0.02 | 0.01 |
| Bemba + Kigoma | 19 | 3.13 | 2.06 | 0.12 | 0.17 | 1.52 | 0.94 | 0.08 | 0.10 |
| TOTALS | 85 | 2.59 | 1.89 | 0.06 | 0.10 | 1.45 | 0.84 | 0.04 | 0.05 |
| **Samples >80 m Depth by Location** | | | | | | | | | |
| Nyanza Lac | 1 | 8.54 | na | 0.36 | na | 3.85 | na | 0.18 | na |
| Ruzizi | 4 | 4.34 | 1.25 | 0.75 | 0.21 | 3.29 | 0.49 | 0.39 | 0.21 |
| Magara | 4 | 2.36 | 0.55 | 0.25 | 0.10 | 2.15 | 0.58 | 0.09 | 0.06 |
| Banza | 11 | 8.40 | 1.14 | 0.57 | 0.18 | 4.88 | 0.52 | 0.55 | 0.17 |
| Bemba | 15 | 3.73 | 2.09 | 0.28 | 0.21 | 3.40 | 2.15 | 0.18 | 0.17 |
| Kigoma | 10 | 8.47 | 1.41 | 0.39 | 0.26 | 3.59 | 0.99 | 0.21 | 0.13 |
| Magara + Banza | 15 | 6.79 | 2.94 | 0.48 | 0.21 | 4.16 | 1.35 | 0.42 | 0.26 |
| Bemba + Kigoma | 25 | 5.62 | 2.98 | 0.32 | 0.23 | 3.23 | 1.76 | 0.19 | 0.16 |
| TOTALS | 45 | 5.96 | 2.90 | 0.41 | 0.25 | 3.69 | 1.55 | 0.29 | 0.22 |

*n = number of samples; SD = standard deviation; TOC = total organic carbon. Note that 80 m approximates the boundary between oxic and anoxic bottom waters. Acid-insoluble sulfur values are used in the subsequent analyses due to problems in using total sulfur from modern sediments because several sources of nonpyritic sulfur exist (Davison, 1988).

site. Carbonate-cemented beachrock (grainstone) commonly forms tabular beds sloping lakeward at up to 5° along the beaches (Cohen and Thouin, 1987). Otherwise, sedimentary structures are limited to rippled sand within the lower shoreface. Elsewhere, clastic-dominated sand facies are limited to small (<100 m long and tens of meters wide) submerged bars directly in front of the Rwaba River and associated lobes of poorly sorted, sandy-silt facies (Table 1) present within the delta-front environment of the Rwaba and Gifuruzi river deltas (Figure 8B).

The most areally significant coarse-grained facies is the coarse- to medium-grained carbonate sand/shell gravel facies [gastropod shell blanket of Cohen and Thouin (1987)] that blankets the shallow bench (Figure 8B). This facies consists of clastic gravel and sand, whole gastropod and bivalve shells, shell fragments, ooids, and silt and would be classified as a bioclastic grainstone upon lithification. The bioclasts consist of the endemic gastropods, *Neothauma tanganyicense*, several species of the genus *Paramalania* sp., and one bivalve genus, *Caelatura*. Because the silt component varies spatially across the bench, this facies would be classified as either a bioclastic grainstone or packstone. Most of the silt is carbonate; however, an increase in silt content adjacent to the Rwaba and Gifuruzi rivers (Figure 9) suggests that reworking of the deltaic deposits also contributes clastic silt to this facies. Patches of *Chara*, common along the bench in water depths of 2–10 m, not only trap silt (Cohen and Thouin, 1987), but also may contribute to the silt component upon breakdown. Ooids, with both tangential and radial fabric, are pervasive in samples from the shoreface down to 38 m, although they are most common in water depths from 2 to 5 m (Cohen and Thouin, 1987; Tiercelin et al., 1992).

A patchy and uneven region of silty sand facies extends across the bench from approximately the Gifuruzi River to the southern end of the study site

**Table 3. Means and Standard Deviations of Rock-Eval Pyrolysis Data for Lake Tanganyika Samples***

| | n | $T_{max}$ (°C) | | Free Bitumen (S1) | | Kerogen Potential (S2) | | $CO_2$ Yield (S3) | | Production Index** | | Hydrogen Index** | | Oxygen Index** | | Quality Index** | |
|---|---|---|---|---|---|---|---|---|---|---|---|---|---|---|---|---|---|
| | | Ave. | SD | Ave. | SD | Ave. | SD | Ave. | SD | Ave. | SD | Ave. | SD | Ave. | SD | Ave. | SD |
| **Means and Standard Deviations for All Samples by Location** | | | | | | | | | | | | | | | | | |
| Nyanza Lac | 13 | 412 | 20 | 0.32 | 0.25 | 1.02 | 0.93 | 1.74 | 0.70 | 0.27 | 0.11 | 99 | 53 | 212 | 97 | 0.50 | 0.29 |
| Ruzizi | 40 | 412 | 8 | 0.26 | 0.21 | 1.19 | 1.15 | 2.32 | 0.78 | 0.19 | 0.03 | 75 | 77 | 184 | 219 | 0.46 | 0.31 |
| Magara | 16 | 410 | 37 | 0.49 | 0.41 | 1.88 | 1.48 | 2.62 | 1.76 | 0.20 | 0.05 | 92 | 36 | 148 | 35 | 0.63 | 0.28 |
| Banza | 13 | 426 | 2 | 2.25 | 0.98 | 9.91 | 4.02 | 4.14 | 1.01 | 0.18 | 0.01 | 223 | 52 | 98 | 18 | 2.35 | 0.72 |
| Bemba | 21 | 416 | 15 | 0.66 | 0.87 | 3.21 | 3.22 | 3.15 | 2.02 | 0.17 | 0.04 | 110 | 85 | 131 | 37 | 0.89 | 0.65 |
| Kigoma | 21 | 420 | 26 | 1.22 | 1.09 | 5.85 | 4.93 | 2.60 | 1.38 | 0.17 | 0.03 | 191 | 103 | 112 | 21 | 1.78 | 1.06 |
| Magara + Banza | 29 | 417 | 29 | 1.28 | 1.14 | 5.48 | 4.96 | 3.30 | 1.64 | 0.19 | 0.04 | 153 | 79 | 125 | 38 | 1.40 | 1.01 |
| Bemba + Kigoma | 42 | 418 | 21 | 0.94 | 1.01 | 4.53 | 4.32 | 2.87 | 1.73 | 0.17 | 0.04 | 150 | 102 | 122 | 31 | 1.34 | 0.98 |
| TOTALS | 124 | 415 | 20 | 0.73 | 0.91 | 3.31 | 4.00 | 2.68 | 1.45 | 0.19 | 0.06 | 121 | 91 | 152 | 134 | 0.98 | 0.89 |
| **Means and Standard Deviations for Samples <80 m Depth by Location** | | | | | | | | | | | | | | | | | |
| Nyanza Lac | 12 | 410 | 21 | 0.30 | 0.25 | 0.85 | 0.73 | 1.65 | 0.65 | 0.28 | 0.11 | 90 | 44 | 214 | 101 | 0.45 | 0.24 |
| Ruzizi | 36 | 411 | 8 | 0.20 | 0.12 | 0.88 | 0.59 | 2.21 | 0.72 | 0.19 | 0.03 | 71 | 80 | 193 | 229 | 0.38 | 0.20 |
| Magara | 12 | 407 | 43 | 0.45 | 0.43 | 1.77 | 1.60 | 2.52 | 2.00 | 0.19 | 0.06 | 89 | 39 | 152 | 40 | 0.60 | 0.28 |
| Banza | 2 | 423 | 1 | 0.96 | 0.70 | 4.14 | 2.98 | 2.13 | 0.85 | 0.19 | 0.00 | 219 | 22 | 128 | 36 | 1.81 | 0.68 |
| Bemba | 7 | 413 | 9 | 0.16 | 0.13 | 0.79 | 0.60 | 1.64 | 0.90 | 0.17 | 0.03 | 50 | 25 | 124 | 15 | 0.43 | 0.17 |
| Kigoma | 11 | 414 | 36 | 0.44 | 0.54 | 2.21 | 2.62 | 1.66 | 1.09 | 0.17 | 0.04 | 114 | 83 | 119 | 25 | 0.98 | 0.78 |
| Magara + Banza | 14 | 410 | 40 | 0.52 | 0.48 | 2.11 | 1.90 | 2.47 | 1.86 | 0.19 | 0.05 | 109 | 60 | 148 | 39 | 0.77 | 0.54 |
| Bemba + Kigoma | 18 | 413 | 28 | 0.33 | 0.44 | 1.66 | 2.16 | 1.65 | 0.99 | 0.17 | 0.04 | 89 | 73 | 121 | 21 | 0.77 | 0.67 |
| TOTALS | 80 | 411 | 23 | 0.30 | 0.33 | 1.27 | 1.44 | 2.05 | 1.08 | 0.20 | 0.06 | 84 | 71 | 172 | 163 | 0.55 | 0.45 |
| **Means and Standard Deviations for Samples >80 m Depth by Location** | | | | | | | | | | | | | | | | | |
| Nyanza Lac | 1 | 429 | na | 0.64 | na | 3.03 | na | 2.83 | na | 0.17 | na | 202 | na | 189 | na | 1.07 | na |
| Ruzizi | 4 | 425 | 2 | 0.72 | 0.24 | 3.96 | 1.35 | 3.35 | 0.64 | 0.15 | 0.01 | 118 | 27 | 101 | 5 | 1.16 | 0.24 |
| Magara | 4 | 417 | 3 | 0.63 | 0.34 | 2.22 | 1.16 | 2.91 | 0.82 | 0.22 | 0.02 | 98 | 33 | 135 | 14 | 0.74 | 0.28 |
| Banza | 11 | 426 | 2 | 2.49 | 0.83 | 10.96 | 3.26 | 4.51 | 0.46 | 0.18 | 0.01 | 224 | 56 | 93 | 6 | 2.45 | 0.71 |
| Bemba | 14 | 418 | 18 | 0.91 | 0.98 | 4.41 | 3.34 | 3.90 | 2.02 | 0.17 | 0.05 | 139 | 89 | 135 | 44 | 1.12 | 0.68 |
| Kigoma | 10 | 426 | 3 | 2.08 | 0.85 | 9.85 | 3.51 | 3.62 | 0.82 | 0.17 | 0.01 | 276 | 21 | 105 | 13 | 2.67 | 0.42 |
| Magara + Banza | 15 | 424 | 5 | 1.99 | 1.12 | 8.63 | 4.89 | 4.08 | 0.91 | 0.19 | 0.02 | 190 | 76 | 104 | 21 | 1.99 | 0.99 |
| Bema + Kigoma | 24 | 421 | 14 | 1.40 | 1.08 | 6.68 | 4.31 | 3.78 | 1.61 | 0.17 | 0.04 | 196 | 97 | 123 | 37 | 1.76 | 0.97 |
| TOTALS | 44 | 423 | 11 | 1.52 | 1.09 | 7.01 | 4.48 | 3.82 | 1.33 | 0.18 | 0.03 | 187 | 86 | 116 | 33 | 1.77 | 0.94 |

*n = number of samples; SD = standard deviation; na = not applicable. Note that 80 m approximates boundary between oxic and anoxic bottom waters.
**Production Index = S1/(S1 + S2); Hydrogen Index = (S2/Total organic carbon) × 100; Quality Index = S2/S3.

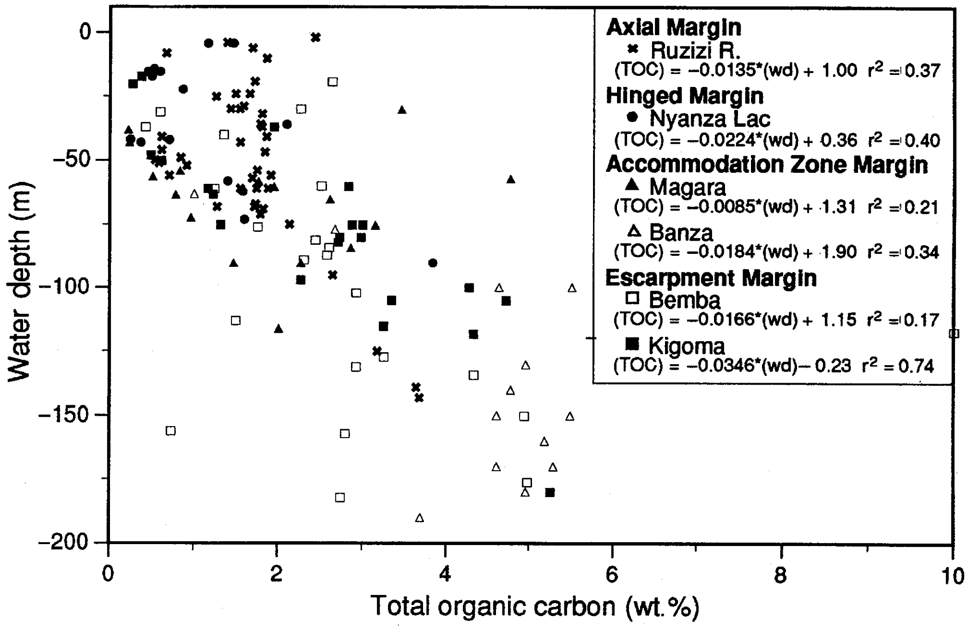


**Figure 6**—Plot of total organic carbon (TOC) vs. water depth (wd) for Lake Tanganyika sediment samples. Data are coded by site. Regression equations are calculated in same manner as in Figure 5.

(Figure 8B). The silt component is highly variable in abundance, but consists mostly of carbonate silt. This facies would be classified as a bioclastic packstone to wackestone because of the abundance of shell fragments and ooids within the sand fraction and up to 5% whole bioclasts. Sedimentary structures within this facies include abundant gastropod grazing tracks and "fish nests" (Cohen and Thouin, 1987). Based on observations from scuba divers, the silty sand facies forms an uneven blanket, 2–10 cm thick, over the carbonate sand/shell gravel facies.

The slope break at the offshore edge of the bench is a rocky, sediment-starved region locally colonized by stromatolites (Cohen and Thouin, 1987). These stromatolites are up to 3 m high and typically are formed by nonlaminated, high-Mg carbonates. Cohen and Thouin (1987) inferred that these stromatolites are relict because they are presently blanketed by a carbonate silt of variable thickness; the stromatolites were subsequently dated by Casanova and Hillaire-Marcel (1992), yielding ages as old as 2950 ±150 yr.

The sublacustrine canyon offshore of the Rwaba River was not sampled. However, a 1.6-m core collected within a sublacustrine canyon along the same hinged margin consists of poorly sorted, coarse-grained, mixed clastic and bioclastic sand and gravel (Tiercelin et al., 1994). This sediment, which is visually identical to the carbonate sand/shell gravel facies, implies that the sublacustrine channels feed deep-water environments with coarse-grained, bioclastic material. Carbonate and clastic silt accumulates as a uniform blanket along the steeper slopes away from the canyons. Massive carbonate mud accumulates in water depths below 60 m; below 90 m, millimeter-scale, white-gray laminated couplets predominate.

### *Organic Composition*

TOC and acid-insoluble sulfur values from the Nyanza Lac site are uniformly low across the shallow-water reaches of the site (Table 2, Figure 6). Spatial variability in organic content along the site is generally minimal, except for the relationship between increasing TOC and increasing water depth (Figure 6). In addition, TOC is 1% higher within the fine-grained deltaic environment of the Rwaba River compared with the coarser grained carbonate sand/shell gravel elsewhere on the bench. Pyrolysis data (Table 3) indicate that the organic matter is consistently lean (low total hydrocarbon potential = S1 + S2) and highly oxidized (low HI:OI ratio; Figure 7).

## Ruzizi River Delta Site: Axial Margin

### *Geomorphology*

The Ruzizi River delta site occupies an area of approximately 50 km$^2$ and lies along an axial margin that cuts across the structural axis of the rift at the northern end of Lake Tanganyika (Figure 3). The site is dominated by the Ruzizi River delta and associated subenvironments (Figure 10A). The Ruzizi River, the second-largest river to enter Lake Tanganyika (drainage area of 5709 km$^2$), originates